

Dust-to-gas Ratio and Metal Abundance in Dwarf Galaxies

U. Lisensfeld¹ & A. Ferrara
Osservatorio Astrofisico di Arcetri
50125 Firenze, Italy
E-mail: ferrara@arcetri.astro.it

ABSTRACT

We have compared the metallicity (represented by oxygen abundance), X_o , and the dust-to-gas ratio, \mathcal{D} , in a sample of dwarf galaxies. For dwarf irregulars (dIrrs) we find a good correlation between the two quantities, with a power-law index 0.54 ± 0.2 . Blue Compact Dwarf (BCD) galaxies do not show such a good correlation; in addition both the dust-to-gas ratio and the metallicity tend to be higher than for dIrrs. We have then developed a simple but physical analytical model for the above relation. Comparing the model results with the data, we conclude that: (i) for low values of \mathcal{D} , the $\mathcal{D} - X_o$ relation is quasi-linear, whereas for higher values the curve strongly deviates from the linear behavior, implying that the commonly used power-law approximation is very poor; (ii) the deviation from the linear behavior depends critically on the parameter χ , the “differential” mass outflow rate from the galaxy in units of the star formation rate, ψ ; (iii) the *shape* of the $\mathcal{D} - X_o$ curve does not depend on ψ , but only on χ ; however, the specific location of a given galaxy on the curve does depend on ψ ; (iv) the BCD metallicity segregation is due to a higher ψ , together with a significant differential mass outflow. Thus, the lack of correlation can be produced by largely different star formation rates and values of χ in these objects.

Subject headings: ISM: abundances; dust, extinction; galaxies: irregulars; galaxies: evolution
galaxies: ISM; infrared: galaxies

1. Introduction

Interstellar dust consists mainly of heavy elements. Therefore a relation between the dust-to-gas ratio and the metallicity of a galaxy can be expected. The simplest argument to derive this dependence comes from Franco & Cox (1986): the authors suggest that the dust-to-gas ratio, \mathcal{D} , is simply $\propto Z$, the metallicity of the gas. However, this assumption might be too simplistic. Furthermore, the dust-to-gas ratio might be expected to depend on the star formation rate.

Dwek & Scalo (1980) have shown that dust injection from supernovae dominates other sources, if indeed grains can form and survive in the ejecta. This has become clear after the SN1987A event, in which dust has been unambiguously detected (Moseley *et al.* 1989, Kosaza, Hasegawa & Nomoto 1989). Indeed, the bulk of the refractory elements (characterized by higher melting temperatures, such as Si, Mg, Fe, Ca, Ti, Al etc.) is injected into the ISM by supernovae (McKee 1989). Dust can be destroyed by interstellar

¹Present address: Universidad de Granada, Departamento de Física Teórica y del Cosmos, 18002 Granada, Spain, E-mail: ute@ugr.es

shocks: small grains are destroyed by thermal sputtering in fast non-radiative shocks; large grains are destroyed by grain-grain collisions and eroded by non-thermal sputtering in radiative shocks (Jones *et al.* 1994, Borkowski & Dwek 1995). In addition, dust grains might be expelled from the galaxy either by radiation pressure (Ferrara *et al.* 1991) or convected away by a fountain-like flow (Norman & Ikeuchi 1989). From these arguments, it follows that the dust content of a galaxy is clearly governed by supernovae, and therefore the equilibrium established between the formation and destruction processes could be influenced by the star formation history of the galaxy.

The aim of this paper is to investigate these processes. As a first step we want to ascertain empirically the existence of a relation between the dust-to-gas ratio, metallicity and the star formation activity. The results are used to constrain a model for the dust production taking into account the processes described above. We have selected dwarf galaxies as objects for this study. The reason is twofold: (i) the metallicities observed in these objects span a large range of values; (ii) due to their small size and simple structure, radial gradients in the dust-to-gas ratio and metallicity can be neglected. Both features make them suitable objects for a comparison of the dust-to-gas ratio and metallicity. The knowledge of the dust content in dwarf galaxies is also relevant to cosmological studies as dwarfs represent the most numerous population of galaxies. Thus a non-negligible fraction of metals in the universe can be locked in such objects, with possible implications for QSO obscuration by dust.

So far only few studies have been concerned with the relation between the dust-to-gas ratio and the metallicity. Issa, MacLaren & Wolfendale (1990) have compared the dust-to-gas ratio and the metallicities in the Galaxy and 6 nearby galaxies and found evidence for a correlation, with the two quantities decreasing at roughly the same rate with increasing galactocentric radius. When taking both quantities at a fixed radius they also obtained a good correlation, following $Z \sim \mathcal{D}^{0.85 \pm 0.1}$. Schmidt & Boller (1993) have compared the dust-to-gas ratio and metallicity of 23 nearby dwarf galaxies and found that the oxygen abundance is $\sim \mathcal{D}^{0.63 \pm 0.25}$, hence in good agreement with Issa *et al.* (1990).

In the present work we have compiled data for dwarf irregular (dIrr) galaxies and blue compact dwarf (BCD) galaxies from the literature and studied the relation between the dust and metal abundance and the star formation rate. For the dIrr sample we confirm the existence of a correlation which is clearly non-linear whereas for the BCD sample no significant correlation could be found. These results allow a theoretical insight on the physics that governs the metal and dust production and on global galactic properties such as the star formation and mass loss history.

2. The samples and the data

We divide the dwarf galaxies in our study into two subsamples: one sample contains dIrr galaxies and the other sample consists of BCDs. In the dIrr sample we include all galaxies of morphological type S(B)m or I(B)m without applying a, in any case arbitrary, luminosity cutoff. The reason for distinguishing between dIrrs and BCDs is their different recent star formation history: BCDs possess spectra very similar to H II regions, and they are believed to be undergoing a starburst. This variable, intense star formation rate in the recent past could affect the relation between the dust and metal abundance, as the time scale for a starburst ($\approx 10^7 - 10^8$ years) is comparable to the time scales relevant for the dust and metal production which is given by the life time of massive stars. Most of the dIrrs, on the other hand, are not in such an extremely intense star forming phase.

In Tab. 1 and 2 the data for the samples are listed. The sample of dIrr consists of 30 galaxies. The

sample size was mainly constrained by the availability of metallicity data. The oxygen abundances, which were chosen as a tracer for the metallicity, were taken from a compilation of Skillman, Kennicutt & Hodge (1989), Hunter, Gallagher & Rautenkranz (1982) and Schmidt & Boller (1993). The latter authors did a similar study to the present one; their sample contains 23 dIrr galaxies and is a subsample of ours. The rest of the data (far-infrared (FIR) fluxes, distance, blue luminosity, HI mass, optical diameter) were taken from the catalogue of Melisse & Israel (1994a) except for NGC 4236 which was not included in their sample. For this galaxy we took the blue magnitude from de Vaucouleurs et al. (1991) (Third Reference Catalogue, RC3) and the HI flux from Huchtmeier & Richter (1989).

The BCD sample contains 19 galaxies. The metallicities and distances and were taken from Kunth & Sèvre (1986) apart from UM 448, for which the metallicity and distance were taken from Terlevich *et al.* (1992). The blue magnitudes and optical diameters are from RC3. The HI fluxes were taken from the catalogue of Huchtmeier & Richter (1989), or, if not listed there, the HI magnitude was taken from RC3 and converted into flux as described in RC3. The FIR fluxes were taken from the IRAS Faint Source Catalogue (1990). The small size of this sample is due to the fact that, although there exist a lot of metallicity data for BCDs in the literature, for most galaxies it was not possible to find simultaneously HI and FIR data. This is partly due to the fact that good spectra which are essential for the determination of metal abundances are mainly obtained for galaxies with a low dust content and therefore often not detected by IRAS.

The HI mass is derived from the HI flux, S_{HI} as:

$$M_{HI} = 2.36 \cdot 10^5 \left(\frac{S_{HI}}{\text{Jy km s}^{-1}} \right) \left(\frac{D}{\text{Mpc}} \right)^2 M_{\odot}. \quad (1)$$

2.1. Calculation of the dust mass

The dust masses were calculated from the FIR emission using a single temperature, black-body model:

$$M_{\text{dust}} = \frac{f_{100} D^2}{B(\nu, T_{\text{dust}}) Q_{\nu}} \quad (2)$$

where $B(\nu, T_{\text{dust}})$ is the Planck emission function, D the distance to the galaxy, f_{100} the IRAS flux at 100 μm and T_{dust} the dust temperature. The infrared dust absorption coefficient, Q_{ν} , is assumed to be the same for all galaxies and was taken from Hildebrand (1983):

$$Q_{\nu} = 0.1 \left(\frac{250}{\lambda} \right)^{\beta} \text{ g/cm}^2; \quad (3)$$

T_{dust} is calculated from the ratio of the IRAS fluxes at 60 and 100 μm . Together this yields:

$$M_{\text{dust}} = 12 \left(\frac{f_{100}}{\text{Jy}} \right) \left(\frac{D}{\text{Mpc}} \right)^2 \left(\frac{250}{100} \right)^{-\beta} \left\{ \left[\frac{f_{100}}{f_{60}} \left(\frac{100}{60} \right)^{\beta+3} \right]^{1.5} - 1 \right\} M_{\odot} \quad (4)$$

We assumed $\beta = 2$. The choice of β has only a minor influence on the dust mass.

2.2. Uncertainties in the dust mass calculation

The dust mass inferred from the FIR emission as described above is affected essentially by two main uncertainties.

First, the value of the dust mass calculated as described above depends sensitively on the dust temperature derived from the 60-to-100 μm flux ratio. We assume hereby that both the 60 and the 100 μm flux is dominated by the emission of big grains, that contain most of the dust mass, and are in thermal equilibrium with the radiation field. If very small grains (VSGs), whose temperature is fluctuating, contribute significantly to the 60 μm emission this method produces wrong results. In the Galactic diffuse, ‘cirrus’, emission the emission of VSGs could indeed contribute significantly to the 60 μm flux (Désert, Boulanger & Puget, 1990) since the dust temperature derived from 60/100 μm ratio stays almost constant in spite of a decreasing radiation field (Sodrowski *et al.* 1987). However, the contribution of VSGs to the 60 μm flux is expected to be only significant in a low radiation field in which the big grains have a low temperature and contribute little to the 60 μm emission (Désert *et al.* 1990). This is not the case for dwarf galaxies which show higher 60/100 μm and lower 12/25 μm ratios than spiral galaxies (Xu & de Zotti 1991, Melisse & Israel 1994b) indicating a lack of ‘cirrus’ emission.

Next, the dust-to-gas ratio derived from the FIR and sub-mm emission is generally significantly, around a factor of 10, lower than the value found in the Solar Neighborhood. This has been found both for simple blackbody models like the present one (Young *et al.* 1989, Devereux & Young 1990) as well as for more detailed dust models (Rowan-Robinson 1992, Andreani & Franceschini 1996). The presence of cold dust, emitting mainly beyond 100 μm , might be responsible for this discrepancy.

Apart from the above arguments, we have carried out the following tests in order to check whether our method is reliable.

1) If the dust temperature derived from the 60 and 100 μm fluxes is a good measure for the real temperature of the big grains, it should correlate with the radiation field. In Fig. 1 the dust temperature and the surface brightness of the bolometric luminosity for both samples are plotted. The bolometric luminosity was calculated as described below and the galaxy surface area is obtained from the optical diameter. A good correlations between the dust temperature and the bolometric surface brightness is visible. The correlation is better for the dIrrs ($r = 0.77$) than for the BCDs ($r = 0.44$). This supports our assumption that the dust temperature represents the temperature of big grains in thermal equilibrium.

2) An alternative way to estimate the dust mass is through an energy balance between the fraction of the radiation absorbed by the dust and escaping from a galaxy (Xu & Buat 1995, Xu & Helou 1996). From the fraction of nonionizing radiation absorbed by the dust we can estimate the dust opacity and from that, assuming that the opacity produced by a certain dust mass is the same as in the Galaxy, the dust mass per area can be calculated. We have calculated the fraction of radiation absorbed by dust following the model of Xu & Buat (1995) who estimate the bolometric luminosity from the ultraviolet (L_{UV}), blue (L_B) and FIR luminosity. For our sample, the ultraviolet (UV) fluxes were available for only 8 galaxies (taken from Deharveng *et al.* 1994, Donas *et al.* 1987, Donas & Deharveng 1984). For these we derived $L_B/L_{UV} = 3.8$ which we use for the whole sample.

The dust is heated both by ionizing photons and by nonionizing photons. Only the dust heating due to nonionizing photons is related to the dust opacity, since we assume that almost all the ionizing photons are absorbed by dust located inside H II regions surrounding massive stars. Of course this assumption can only represent a first approximation, since some ionizing photons will escape into the diffuse ISM (Beckman, private communication). Thus, in order to calculate the dust opacity we have to subtract the dust heating by ionizing photons. We estimate the ionizing UV radiation from the H_α emission. The total H_α fluxes were available for a large part of the dIrr sample (19 galaxies, H_α fluxes taken from Hunter, Hawley & Gallagher 1993, Hunter *et al.* 1989, Kennicutt & Kent 1983). Since the dust opacity is generally low in dwarf galaxies,

the extinction of the H_α line is likely to be small and we neglected it. The total dust emission originating from ionizing radiation can be estimated as $f_{\text{dust}}^{\text{lyc}} = 27.12 \times f_{H_\alpha}$ (Xu & Buat 1995). The average fraction of dust emission due to heating by ionizing photons is $f_{\text{dust}}^{\text{lyc}}/f_{\text{dust}} = 0.45 \pm 0.35$, where f_{dust} is the total dust emission, extrapolated from the FIR emission according to Xu & Buat (1995). We use this average value for the galaxies for which no H_α data is available.

The dust opacity is estimated using a simplified radiation transfer model with a slab geometry, assuming that dust and stars are homogeneously mixed. We use an approximate formula (Xu & de Zotti 1989) for the dust absorption probability, further simplified by dividing the nonionizing radiation into two (optical and UV) bands for which we take the extinction properties at 4300 Å and 2000 Å, respectively (see Lisenfeld, Völk & Xu 1996).

The opacities deduced (at 4300 Å), τ_B , range between 0.01 and 0.4. Assuming that the dust has the same extinction properties as dust in our Galaxy (Désert *et al.* 1990), we can estimate the dust mass as

$$M_{\text{dust}}^{\text{opa}} [M_\odot] = 8.8 \cdot 10^4 \times \tau_B \times \left(\frac{A_{\text{gal}}}{\text{kpc}^2} \right) \quad (5)$$

where A_{gal} is the optical surface area of the galaxy. In Fig. 2 the dust mass estimated in this way and the dust mass calculated from the FIR emission are compared. The most striking result is the very good ($r = 0.96$) and practically linear (slope = 1.09 ± 0.04) correlation between the two quantities. The dust mass derived from the FIR emission is on average a factor of 25 lower than the mass derived from the opacity. However, since the main aim of the present work is the comparison of the dust-to-gas ratio with the metallicity of galaxies, the absolute value of the dust mass is only of secondary importance; the crucial point is that the *ratio* of the dust masses is correct. The linear correlation between the dust masses derived in two different ways (from the FIR emission and from the extinction) corroborates that this latter assumption is correct.

3. Comparison of the dust-to-gas ratio and the metallicity

In Fig. 3 - 5 the dust-to-gas ratios and the metallicities are plotted for the two samples. For the 4 galaxies in the dIrr sample with upper limits in both IRAS fluxes, the dust temperature is undefined and therefore, strictly speaking, the dust mass as well. Since the dust temperature in the sample shows a small dispersion (all values lie between 22 and 42 K) we adopted a $T = 30$ K for these 4 galaxies and calculate the dust mass with this value in order to give at least an indicative value (filled squares in Fig. 3 and 5).

We only considered the H I gas mass in our analysis. We could not derive H_2 masses for the whole sample because of the lack of data. Since the H I / H_2 mass ratio in dwarf galaxies is in general very high (Young & Knezek 1989, Schmidt & Boller 1993) we expect that the error produced by this is only small. For 11 galaxies of our sample we could find CO data in the literature (Young *et al.* 1995, Elfhag *et al.* 1996) and we derived the H_2 mass using the standard CO-to- H_2 conversion factor ($M_{H_2} = 4.78 L_{CO}$). For 8 of them we found $M_{H_2}/M_{HI} < 0.1$ and only for 3 galaxies – all of them BCDs – this ratio is ~ 1 or larger. The largest mass ratio was found for NGC 3690 with $M_{H_2}/M_{HI} = 8$. A further uncertainty is, however, the question whether the conversion factor between H_2 and CO is the same in dwarf galaxies as in spirals. There are theoretical (Maloney & Black 1988) and observational indications (Ohta *et al.* 1993, Verter & Hodge 1995) that it might be higher in the low metallicity ISM of dwarf galaxies. It is not possible at the moment to assess the possible error caused by neglecting molecular gas.

For the dIrr sample there exists a good correlation between the dust-to gas ratio and the metallicity (Fig. 3). The correlation coefficient is (not taking into account the 4 galaxies with only upper limits in the FIR) $r = 0.52$ and, not taking into account either the two galaxies (DDO 168 and GR8) that are clearly off the correlation, it increases to $r = 0.80$. The correlation is not linear; a least square fit yields: $12+\log(\text{O}/\text{H}) \propto \log(M_{\text{dust}}/M_{\text{HI}})^{0.54 \pm 0.2}$. This result is in agreement with earlier studies: Schmidt & Boller (1993) obtained a very similar slope in the correlation as we (0.63 ± 0.25) which is to be expected because our sample is an extension (7 more galaxies) of theirs. The results of Issa *et al.* (1990) who compared the dust-to-gas ratio in nearby galaxies are similar. From their data a slope of 0.85 ± 0.1 can be obtained (Schmidt & Boller 1993).

The sample of the BCDs shows no obvious correlation between the dust-to-gas ratio and the metallicity (Fig. 4). The correlation coefficient is $r = 0.25$ (again only taking into account galaxies with FIR detections), however it increases to $r = 0.5$ if we neglect the galaxy (NGC 3690) which is clearly off the correlation. For NGC 3690 we found a very high H_2/HI mass ratio, as mentioned above: this might be the reason for the peculiar behavior of this galaxy. Both the average dust-to gas ratio as well as the average metallicity are higher for this sample than for the dIrrs (Fig. 5). For a given metallicity the dust-to-gas ratio is on average higher than for the dIrr galaxies.

4. Model

We are now interested in developing a simple model that explains the observed behavior of the dust-to-gas/metallicity relation in dwarf galaxies. In particular one would like to understand (i) the physics that governs the observed relationship (ii) the apparently different trend found in dIrrs and BCDs (iii) learn about star formation, metal production, and mass loss history of these objects.

4.1. Basic Equations

To answer the above questions, we start writing the equations describing the rate of change of the galactic gas mass, M_g , the mass fraction of a given heavy element i , denoted by $X_i = M_i/M_g$ (M_i is the mass of the element i), and the ratio between the mass in element i and the dust mass, $f = M_d/M_i = M_d/X_iM_g$:

$$\frac{d}{dt}M_g = -\psi + E - W, \quad (6)$$

$$\frac{d}{dt}M_i = \frac{d}{dt}[X_iM_g] = -X_i\psi + E_i - X_iW, \quad (7)$$

$$\frac{d}{dt}M_d = \frac{d}{dt}[fX_iM_g] = -\alpha f X_i\psi + f_{in}E_i - \frac{fX_iM_g}{t_{sn}} - \delta f X_iW. \quad (8)$$

We now discuss in detail the various quantities entering eqs. 6-8. The star formation rate (SFR) is denoted by ψ ; E is the total injection rate from stars of all masses and ages; E_i is the total injection rate of element i from stars; W is the net outflow rate from the galaxy. The three parameters in eq. 8 α , f_{in} and δ refer to dust properties: αf is the fraction of dust destroyed during star formation ($\alpha = 1$ corresponds to destruction of only the dust incorporated into the star, $\alpha > 1$ [$\alpha < 1$] corresponds to a net destruction [formation] in the protostellar environment); f_{in} is the value of the dust fraction in the injected material; δ accounts for a possible different dust content of the outflow with respect to the general interstellar medium

($\delta = 0 \Rightarrow$ no dust in the outflow; $\delta = 1 \Rightarrow$ the outflow is as dusty as the ISM). It is easy to understand the physical meaning of the above equations from an inspection of the various terms. Eq. 6 and 7 describe the detailed balance of the gas and i -element mass as due to star formation, stellar injection and outflows; eq. 8 accounts for the fact that dust is destroyed/formed during star formation processes, it is injected by stellar sources, destroyed by supernova shocks (on a characteristic time-scale t_{sn}) and lost in outflows. We have neglected the change of M_i deriving from grain destruction in comparison with the stellar metal production; this approximation holds for values $\mathcal{D} \lesssim 10^{-3}$ and therefore should be appropriate for our sample; also eq. 8 does not take into account the possible formation or accretion of dust directly in the interstellar medium. The validity of this assumption is difficult to assess, since the determination of the grain accretion rate in the ISM would require a detailed knowledge of the grain microphysics. However, since accretion is well known to occur preferentially in high gas density regions (molecular clouds), we hope that this process, due to the paucity of molecular gas in dwarfs galaxies, will not have a dramatic impact on our results.

We next adopt the *Instantaneous Recycling Approximation*, (IRA) *i.e.* stars less massive than $1 M_\odot$ live forever and the others die instantaneously, (Tinsley 1980) which allows E and E_i to be written respectively as

$$E = R\psi; \quad E_i = [RX_i + y(1 - R)]\psi, \quad (9)$$

(Note that Tinsley’s eq. 3.14 contains a wrong extra factor $1 - X_i$, see Maeder 1992), where R and y are the standard returned fraction (the fraction of the total mass that has formed stars which is subsequently going to be ejected into the ISM) and net stellar yield (the total mass of an element i ejected by all stars back into the ISM per unit mass of matter locked into stars), respectively. The limitations of IRA are discussed in Tinsley (1980). Moreover, we assume that the outflow rate is $W = w\psi$, with $w = \text{const.}$, a common *ansatz* in chemical evolution models. It is also useful for our purpose to write the above equations in terms of the dust-to-gas ratio, $\mathcal{D} = f X_i$. With these positions, eqs. 6-8 become

$$\frac{1}{\psi} \frac{d}{dt} M_g = (R - 1 - w) \quad (10)$$

$$\frac{M_g}{\psi} \frac{d}{dt} X_i = y(1 - R) \quad (11)$$

$$\frac{M_g}{\psi} \frac{d}{dt} \mathcal{D} = -[R - 1 - w(1 - \delta) + \alpha] \mathcal{D} + f_{in}[RX_i + y(1 - R)] - \frac{M_g}{t_{sn}} \frac{\mathcal{D}}{\psi} \quad (12)$$

To determine t_{sn} we follow McKee (1989), who writes this quantity as

$$t_{sn} = \frac{M_g \gamma^{-1}}{\bar{\epsilon} M_s (100)} \quad (13)$$

where γ is an “effective” supernova rate calculated including both Type II and Type I supernovae and accounting for the fact that not all the SNRs interact with the galactic ISM. For sake of simplicity, and also because the second effect should be less important in small objects like dwarf galaxies, we neglect these complications and take γ as the Type II SN rate. We write $\gamma = \nu\psi$, where ν is the number of supernovae per unit stellar mass formed. We assume ν to be the same as in the Galaxy, for which $\psi \sim 3 M_\odot \text{ yr}^{-1}$ (Larson 1996) and $\gamma \sim 0.022 \text{ yr}^{-1}$ (van den Bergh 1983); this yields $\nu = 1/136 M_\odot = 3.610^{-36} \text{ g}^{-1}$. The mean efficiency of grain destruction by a shock is denoted by $\bar{\epsilon}$; its precise value depends on the mean gas density and magnetic field strength in the ambient medium. Lacking a precise determination of these quantities in dwarf galaxies, we adopt the conservative value $\bar{\epsilon} = 0.1$, suggested by McKee (1989) for the

Galaxy. Next we need an estimate for $M_s(100)$, the gas mass shocked to a velocity of at least 100 km s^{-1} . From the Sedov-Taylor solution in an homogeneous medium one can easily obtain:

$$M_s(100) = 6800 \left(\frac{E}{10^{51}} \right) \left(\frac{v_s}{100 \text{ km s}^{-1}} \right)^{-2} M_\odot \quad (14)$$

where E is the energy release by the explosion and v_s is the shock velocity. We adopt the fiducial value 100 km s^{-1} in eq. 14 according to McKee (1989). In conclusion, we have

$$t_{sn} = \frac{M_g}{\beta \psi} \quad (15)$$

with $\beta = \bar{\epsilon} \nu M_s(100) \sim 5$.

Since we are interested in the relation between X_i and \mathcal{D} in order to compare it with the data, we eliminate time from the previous equations. This yields

$$\frac{d\mathcal{D}}{dX_i} + a\mathcal{D} - bX_i = c, \quad (16)$$

where

$$a = \frac{[R - 1 - w(1 - \delta) + \alpha + \beta]}{y(1 - R)}, \quad b = \frac{f_{in}R}{y(1 - R)}, \quad c = f_{in}. \quad (17)$$

The solution of eq. 16 is

$$\mathcal{D}(X_i) = \frac{b}{a}X_i + (1 - e^{-aX_i})\left(\frac{c}{a} - \frac{b}{a^2}\right) \quad (18)$$

In order to quantify the above relation, we need to fix the value of R and y for the traced heavy element. We choose oxygen for the following reasons: (i) it is produced mainly in Type II SNe, which are also the ones responsible for the grain shock destruction; (ii) oxygen is the main constituent of grains (the relative abundances of atoms of O:C:Si:Mg in grains are 100:54:6.5:5.2); (iii) a large sample of dwarf galaxies for which good quality abundance data for this species is available (see Sect. 2). We therefore take $X_i \equiv X_o$, the oxygen mass fraction. The returned fraction and the net yield can be obtained using the standard formulae (Maeder 1992):

$$R = \frac{\int_{m_l}^{m_u} (m - w_m)\phi(m)dm}{\int_{m_l}^{m_u} m\phi(m)dm}; \quad y = \frac{1}{(1 - R)} \frac{\int_{m_l}^{m_u} m p_m \phi(m)dm}{\int_{m_l}^{m_u} m\phi(m)dm} \quad (19)$$

where $\phi(m)$ is the initial mass function (IMF) defined between the lower and upper masses $m_l = 1M_\odot$ and $m_u = 120M_\odot$, and w_m ($w_m = 0.7M_\odot$ for $m \leq 4M_\odot$ and $w_m = 1.4M_\odot$ for $m > 4M_\odot$) is the remnant mass (white dwarf or neutron star). We have used a power law form of the IMF, $m\phi(m) \propto m^{-x}$ with $x = 1.35$ (standard Salpeter) and $x = 1.7$ (Scalo 1986). We have taken the oxygen stellar yield, p_m (*i.e.* the mass fraction of a star of mass m converted into oxygen and ejected) from Arnett (1990). With these assumptions we obtain $R = (0.79, 0.684)$ and $y = (0.0124, 0.0047)$ for the (Salpeter, Scalo) IMFs, respectively.

4.2. Model Results

Once R and y have been fixed, the solution given by eq. 18 contains four free parameters: $\alpha, f_{in}, w, \delta$. However, the solution is quite insensitive to α : we take it equal to unity. Thus, we are left with three free parameters. The precise value of f_{in} , the dust-to-O mass ratio in stellar dust sources, is rather uncertain;

a simple estimate can be obtained as follows. A typical SN ejects $\sim 4M_{\odot}$ of heavy elements into the ISM. However, only the fraction of oxygen (which dominates the ejected material) that can bind to refractory elements can go into grains, at most 25% as derived from ISM depletion studies. In addition a rather optimistic upper limit for the efficiency of grain formation (largely unknown) is $\sim 40\%$. Thus, $f_{in} \leq 0.1$, but likely to be typically smaller than this value. Given our present ignorance of the processes governing dust formation, we will explore below (see Fig. 7) the effects of varying f_{in} within a range of reasonable values. For the last two free parameters, which describe the outflow process, *i.e.* w and δ , the outflow rate (in units of the SFR) and the dust fractional content of the outflow, we take $0 < w < 20$ and $0 < \delta < 1$ in order to cover a reasonably large parameter space. Fig. 6 shows the main results of this Section. There we plot the solutions for different values of w and δ and compare them with the data points corresponding to the dust-to-gas vs. metallicity relation shown in Fig. 5. The model results are shown for both a Salpeter (solid lines) and a Scalo (dashed) IMF. Several interesting points can be made from an inspection of this Fig. 6.

First, we conclude that a simple power-law does not represent a good fit to the data, but a more much physically meaningful functional is the one given by eq. 18. For low values of \mathcal{D} the relation is shown to be quasi-linear, whereas for higher values the shape of the curve depends sensitively on δ and w , through the coefficient a in eq. 18. In general, for a fixed value of δ , a higher value of the outflow rate produces a flatter curve; the same effect can be obtained by decreasing δ : both situations allow the system to retain a larger fraction of dust. However, the solutions only depend on the product $\chi = w(1 - \delta)$, as can be seen from the coefficient a in eq. 17; χ can be interpreted as a “differential” outflow rate.

Next, we note that the $\mathcal{D} - X_o$ relation *does not* depend on the particular SFR ψ of the galaxy: this could be expected since both metal and dust production are strictly connected implying that the relation found is rather general; however, if all the parameters are constant in time, a given galaxy is forced to move along the appropriate curve as it gets metal and dust enriched. The curves are moderately sensitive to the IMF, with the Scalo IMF covering a larger region of the $\mathcal{D} - X_o$ plane for the given set of parameters.

The results also point out the importance of outflows for dwarf galaxies. The effect of mass loss is particularly evident in the high- \mathcal{D} part of the curves where it results in a flattening; the data require that most of the dwarfs in the sample must have undergone a substantial outflow episode. The segregation of BCDs in the high metallicity, high dust-to-gas ratio region of the plane can be then explained by a higher SFR with respect to dIrrs, which implies a more substantial enrichment in metals and dust. Support to this hypothesis is lent by the fact that BCDs are all consistent with large values (> 20) of the differential outflow rate χ , since ultimately the SFR determines the rate of SNe powering the wind.

Some uncertainty affects the low- \mathcal{D} , low- X_o part of the curves which is sensitive to the precise value of f_{in} , as shown by Fig. 7 for the Scalo IMF. In the limit $X_i \rightarrow 0$, eq. 18 reduces to $\mathcal{D}(X_i) \simeq cX_i = f_{in}X_i$, *i.e.* the solution scales linearly with f_{in} , which we have allowed to vary in $0.003 \leq f_{in} \leq 0.1$. Thus the precise value of f_{in} could be possibly constrained by observations of extremely metal poor objects.

5. Summary and Conclusions

We have compared the metallicity and the dust-to-gas ratio in a sample of 49 (30 dIrr + 19 BCD) dwarf galaxies. The dust mass has been derived from the FIR emission assuming that the dust composition is the same for all galaxies. We have carried out various tests in order to check the reliability of this dust mass determination. For the sample of dIrr galaxies we found a good correlation between the two quantities,

obeying the empirical relation $12+\log(\text{O}/\text{H}) \propto \log(M_{\text{dust}}/M_{\text{HI}})^{0.54\pm 0.2}$. For BCD galaxies we did not find such a good correlation; both the dust-to-gas ratio and the metallicity tend to be higher than in the dIrr sample, and for a given metallicity the dust-to-gas ratio is on average higher than for the dIrr galaxies.

We have derived a simple analytical form for the expected dust-to-gas ratio vs. metallicity, $\mathcal{D} - X_{\text{o}}$, relation (we have assumed that oxygen is a good metallicity indicator) and compared it with the observational data. The main results are the following:

- For low values of \mathcal{D} the $\mathcal{D} - X_{\text{o}}$ relation is shown to be quasi-linear, whereas for higher values the curve strongly deviates from the linear behavior.
- The deviation from the linear behavior depends critically on the parameter $\chi = w(1 - \delta)$, the “differential” mass outflow rate from the galaxy in units of the SFR ψ , and is negative if $\chi < 5$. Most of the galaxies in the sample can then be inferred to have undergone a substantial outflow episode.
- The *shape* of the $\mathcal{D} - X_{\text{o}}$ curve does not depend on the SFR, ψ , of the galaxy but only on the outflow rate; however, the specific location of a given galaxy on the curve does depend on ψ .
- The BCD metallicity segregation is due to a higher SFR, also suggested by their consistency with the generally larger values of the outflow rates required. The lack of correlation could then be produced by largely different star formation rates and values of χ in these objects.

We would like to thank E. Dwek and C. Xu for helpful and interesting discussions. U. L. gratefully acknowledges the receipt of a grant by the Deutsche Forschungsgemeinschaft (DFG) and by the Ministerio de Educación y Ciencia (Spain).

REFERENCES

- Andreani, P. & Franceschini, A. 1996, MNRAS, 283, 85
- Arnett, D. W. 1990, in Chemical and Dynamical Evolution of Galaxies, eds. F. Ferrini *et al.* (Pisa: ETS), 409
- Borkowski, K. J. & Dwek, E. 1995 ApJ, 454 254
- Deharveng, J. M., Sasseen, T. P., Buat, V., Bowyer, S., Lampton, M. & Wu, X. 1994, A&A, 289, 715
- Désert, F. X., Boulanger, F. & Puget, J. L. 1990, A&A, 237, 215
- de Vaucouleur, G., de Vaucouleur, A., Corwin H., *et al.*, 1991, Third Reference Catalog of Galaxies, (New York: Springer) (RC3)
- Devereux, N. A. & Young, J. S. 1990, ApJ, 359, 42
- Donas, J. & Deharveng, J. M. 1984, A&A, 140, 325
- Donas, J., Deharveng, J. M., Laget, M., Milliard, B. & Huguenin, D. 1987, A&A, 180, 12
- Dwek, E. & Scalo, J. M. 1980, ApJ, 239, 193
- Elfhag, T., Booth, R. S., Höglund, B., Johansson, L. E. B., Sandqvist, Aa. 1996, A&AS, 115, 439
- Ferrara, A., Ferrini, F., Franco, J., & Barsella, B. 1991, ApJ, 381, 137
- Franco, J. & Cox, D. P. 1986, PASP, 98, 1076
- Hildebrand, R. H. 1983, QJRAS, 24, 267

- Huchtmeier, W. K. & Richter O.-G. 1989, *A General Catalogue of HI Observations of Galaxies*, (New York: Springer)
- Hunter, D. A., Gallagher, J. S. & Rautenkranz, D. 1982, *ApJS*, 49, 53
- Hunter, D. A., Gallagher, J. S., Rice W. L., & Gillett, F. C. 1989, *ApJ*, 336, 152
- Hunter, D. A., Hawley, W. N. & Gallagher, J. S. 1993, *AJ*, 106, 1797
- Jones, A. P., Tielens, A. G. G. M., Hollenbach, D. J. & McKee, C. F., 1994, *ApJ*, 433, 797
- IRAS Faint Source Catalog, 1990, Version 2.0, Moshir M. *et al.* Infrared Processing and Analysis Center
- Issa, M. R., MacLaren, I. & Wolfendale, A. W. 1990, *A&A*, 236, 237
- Kennicutt, R. C. & Kent, S. M. 1983, *AJ*, 88, 1094
- Kozasa, T, Hasegawa, H. & Nomoto, K. 1989, *ApJ*, 344, 325
- Kunth, D. & Sèvre, F. 1986, in *Star forming dwarf galaxies and related objects*, eds. Kunth, Thuan & Tran-Thanh, (Gif-sur-Yvette: Frontière)
- Larson, R. B. 1996, in *The Interplay between Massive Star Formation, the ISM and Galaxy Evolution*, 11th IAP Meeting, eds. D. Kunth *et al.* (Gif-sur-Yvette: Frontière), 3
- Lisenfeld, U., Völk, H.J. & Xu, C. 1996, *A&A*, 306, 677
- Maloney, P.& Black, J.H. 1988, *ApJ*, 325, 389
- Maeder, A. 1992, *A&A*, 265, 105
- McKee, C. F. 1989, in *Interstellar Dust*, IAU Symp. 135, eds. L. J. Allamandola & A. G. G. M. Tielens, (Dordrecht: Kluwer), 431
- Melisse, J. P. M. & Israel, F. P. 1994a, *A&AS*, 103, 391
- Melisse, J. P. M. & Israel, F. P. 1994b, *A&A*, 285, 51
- Moseley, S. H., Dwek, E., Glaccum, W., Graham, J. R., Loewenstein, R. F. & Silverberg, R. F. 1989, *Nature*, 340, 697
- Norman, C. A. & Ikeuchi, S. 1989, *ApJ*, 345, 372
- Ohta, K., Tomita, A., Saito, M., Sasaki, M. & Nakai, N. 1993, *PASJ*, 45, L21
- Rowan-Robinson, M. 1992, *MNRAS*, 258, 787
- Scalo, J. M. 1986, *Fund. Cosm. Phys.*, 11, 1
- Schmidt K. H. & Boller T. 1993, *Astron. Nachr.*, 314, 361
- Skillman, E. D., Kennicutt, R.C. & Hodge, P. W. 1989, *ApJ*, 347, 875
- Sodroski, T.J., Dwek, E., Hauser, M. G. & Kerr, F.J. 1987, *ApJ*, 322, 101
- Tavelich, R., Melnick, J., Masegosa, J. & Moles, M. 1992, *A&AS*, 91, 285
- Tinsley, B. M. 1980, *Fund. Cosm. Phys.*, 5, 287
- van den Bergh, S. 1983, *PASP*, 95, 388
- Verter, F. & Hodge, P. 1995, *ApJ*, 446, 616
- Xu, C. & de Zotti G. 1989, *A&A*, 225, 12
- Xu, C.& Buat, V. 1995, *A&A*, 293, L65
- Xu, C.& Helou, G. 1996, *ApJ*, 456, 163

Young, J. S. & Knezek, P.M. 1989, ApJ, 347, L55

Young, J. S., Xie, S., Kenney, J. D. & Rice W. L. 1989, ApJS, 261. 492

Young, J. S, *et al.* 1995, ApJS, 98, 219

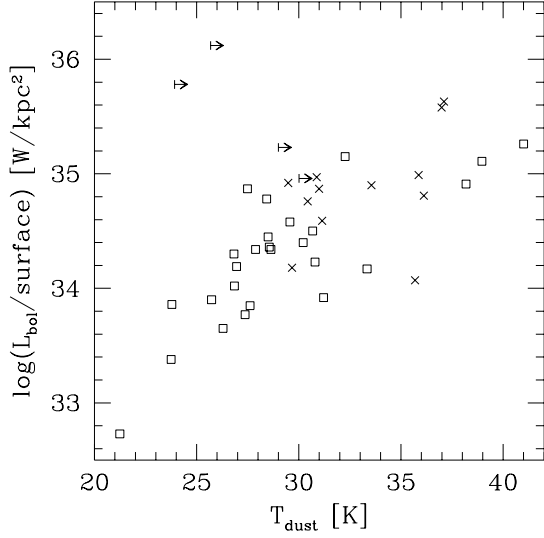


Fig. 1.— Bolometric surface brightness vs. dust temperature for both samples. The crosses denote BCDs with FIR detections, the arrows BCDs with upper limits in the FIR and the open squares dIrr galaxies with FIR detections.

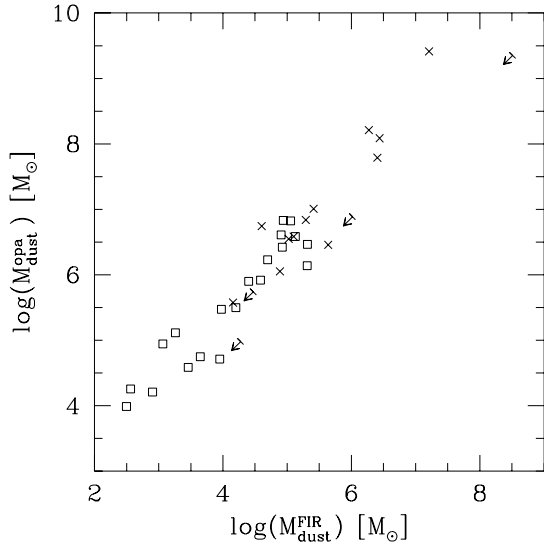


Fig. 2.— Dust masses calculated from the 60 and 100 μm fluxes ($M_{\text{dust}}^{\text{FIR}}$) and from the opacity ($M_{\text{dust}}^{\text{opa}}$). The symbols are defined as in Fig. 1.

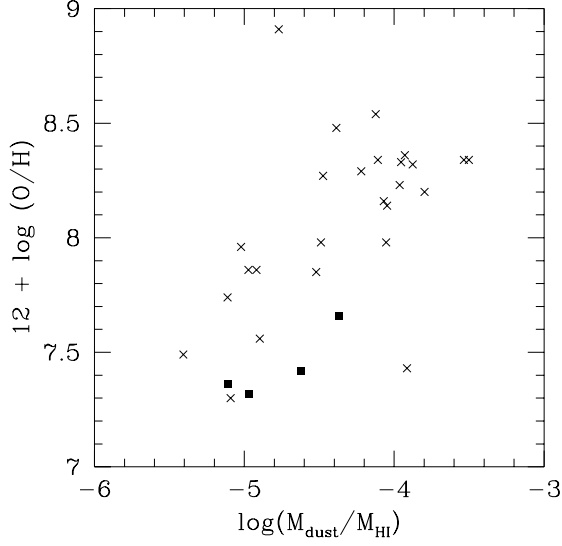


Fig. 3.— Dust-to-gas-ratio and metallicity for the dIrr sample. Filled squares denote galaxies for which M_{dust} is undetermined and only an indicative value is plotted (see text).

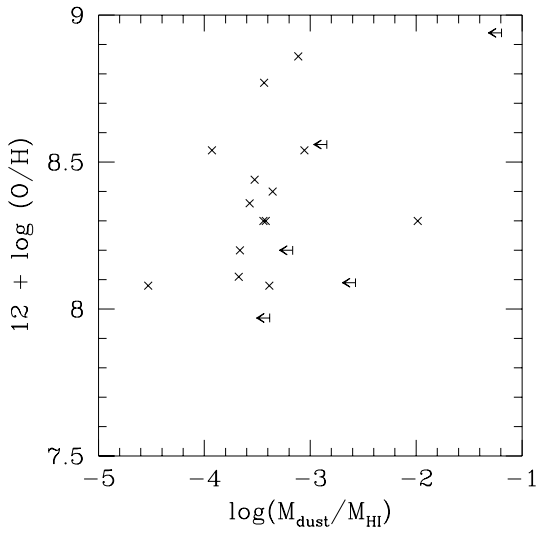


Fig. 4.— Dust-to-gas-ratio and metallicity for the BCD sample. The arrows denote upper limits.

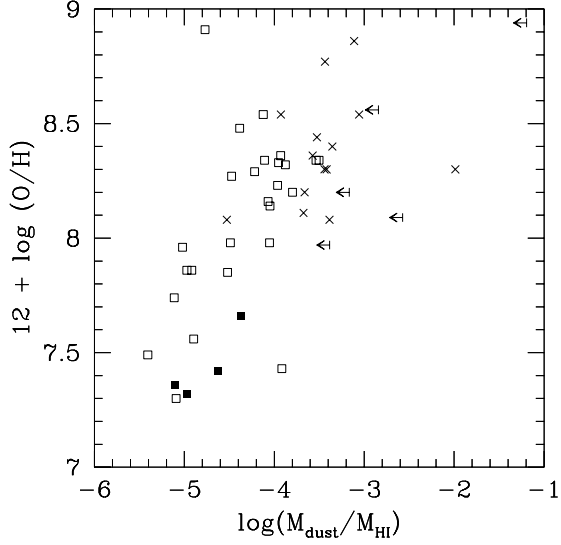


Fig. 5.— Dust-to-gas-ratio and metallicity for both samples (dIrrs and BCDs) together. The symbols are defined as in Fig. 1 and 3

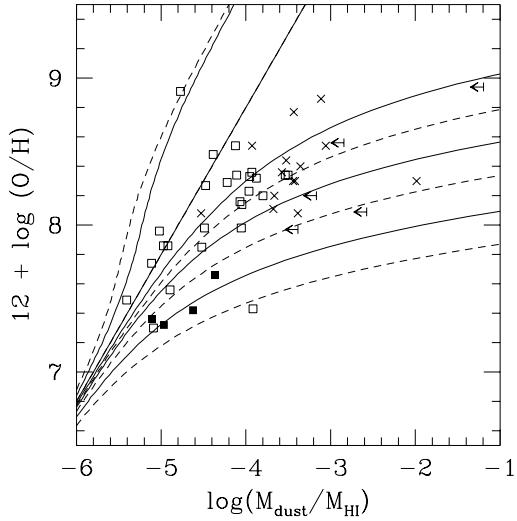


Fig. 6.— Comparison between the theoretical $\mathcal{D} - X_o$ curves given by eq. 18 and data points for the entire sample (symbols as in Fig. 1 and 3). Solid curves refer to Salpeter IMF, dashed curves refer to Scalo IMF. Each set curves is plotted for $f_{in} = 0.01$ and the following values of $\chi = w(1 - \delta) = 0, 5, 7, 10, 20$, from top to bottom.

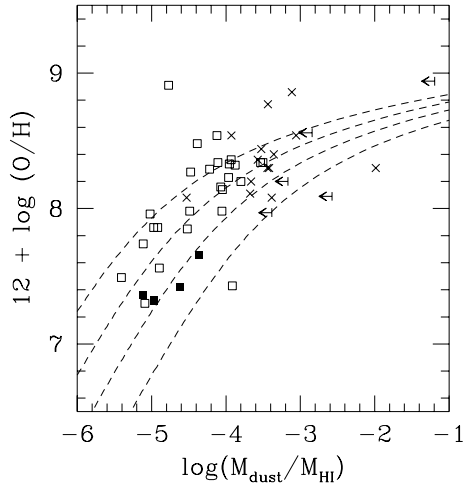


Fig. 7.— Comparison between the theoretical $\mathcal{D} - X_o$ curves given by eq. 18 and data points for the entire sample (symbols as in Fig. 1 and 3) for different values of $f_{in} = 0.1, 0.03, 0.01, 0.003$, from bottom to top, a Salpeter IMF and a fixed value of $\chi = 7$.

Table 1: Data of the dwarf irregular sample

Name	D [Mpc]	f_{60} [Jy]	f_{100} [Jy]	$\log(M_{\text{dust}})$ [M_{\odot}]	$\log(M_{\text{HI}})$ [M_{\odot}]	$\log(\frac{M_{\text{dust}}}{M_{\text{HI}}})$	$12 + \log(O/H)$
SDIG	2.90	< 0.093	< 0.159	2.42	7.04	-4.62	7.42
UGC 4483	4.00	< 0.079	< 0.149	2.73	7.70	-4.97	7.32
DDO 167	3.50	< 0.093	< 0.183	2.73	7.10	-4.37	7.66
DDO 187	2.60	< 0.084	< 0.134	2.20	7.31	-5.11	7.36
GR 8	2.20	0.020	0.143	3.06	6.98	-3.92	7.43
Leo A	1.60	0.090	0.270	2.50	7.59	-5.09	7.30
WLM	1.00	0.320	1.040	2.73	7.84	-5.11	7.74
IC 5152	3.00	2.461	6.861	4.40	8.33	-3.93	8.36
IC 1613	0.70	1.420	3.690	2.82	7.74	-4.92	7.86
Sex A	1.50	0.503	0.849	2.56	7.97	-5.41	7.49
Sex B	1.70	0.246	0.684	2.90	7.80	-4.90	7.56
NGC 6822	0.50	47.630	95.420	3.77	7.82	-4.05	8.14
DDO 47	2.00	0.125	0.555	3.26	7.78	-4.52	7.85
IC 10	2.60	31.230	71.250	5.16	8.96	-3.80	8.20
NGC 2366	3.30	3.303	4.578	3.85	8.87	-5.02	7.96
SMC	0.06	6688.910	15021.930	4.20	8.69	-4.49	7.98
NGC 1569	2.20	39.223	31.748	3.98	8.05	-4.07	8.16
LMC	0.05	82917.000	184686.690	5.13	8.63	-3.50	8.34
NGC 4214	4.10	14.470	25.470	4.94	9.05	-4.11	8.34
NGC 4449	3.90	14.762	37.806	5.31	9.19	-3.88	8.32
NGC 3510	8.90	0.598	1.457	4.58	8.97	-4.39	8.48
NGC 3738	4.20	1.290	2.410	3.98	8.10	-4.12	8.54
NGC 5253	6.90	30.510	29.360	5.06	8.59	-3.53	8.34
DDO 168	3.90	0.268	0.736	3.65	8.42	-4.77	8.91
NGC 55	2.00	77.000	174.100	5.32	9.27	-3.95	8.33
NGC 1156	6.50	5.170	9.200	4.91	8.87	-3.96	8.23
IC 2574	2.40	2.410	10.620	4.70	8.75	-4.05	7.98
NGC 5408	4.20	2.360	2.160	3.46	8.43	-4.97	7.86
IC 4662	2.20	7.360	11.230	3.95	8.17	-4.22	8.29
NGC 4236	4.90	3.980	10.020	4.92	9.40	-4.48	8.27

Table 2: Data of the Blue Compact Dwarf sample

Name	D [Mpc]	f_{60} [Jy]	f_{100} [Jy]	$\log(M_{\text{dust}})$ [M_{\odot}]	$\log(M_{HI})$ [M_{\odot}]	$\log(\frac{M_{\text{dust}}}{M_{HI}})$	$12 + \log(O/H)$
UM 448	76.00	4.140	4.321	6.36	9.75	-3.39	8.08
Mrk 7	42.30	0.480	0.970	5.64	9.57	-3.93	8.54
Mrk 33	21.60	4.680	5.300	5.41	8.77	-3.35	8.40
Mrk 35	14.50	4.950	6.740	5.29	8.73	-3.44	8.30
NGC 3690	40.80	103.700	107.400	7.21	9.20	-1.99	8.30
Mrk 432	45.60	3.890	6.710	6.44	9.88	-3.44	8.77
IC 3258	21.20	0.490	0.970	5.03	8.55	-3.53	8.44
NGC 4670	12.10	2.630	4.470	5.10	8.52	-3.42	8.30
NGC 4861	12.90	1.970	2.260	4.60	9.13	-4.53	8.08
IIZw 70	17.60	0.710	1.240	4.89	8.56	-3.67	8.11
Mrk 296	65.30	0.610	1.440	6.29	9.35	-3.06	8.54
NGC 6764	32.00	6.330	11.560	6.41	9.52	-3.11	8.86
IIIZw 107	73.70	1.370	1.720	6.06	9.72	-3.66	8.20
NGC 7714	40.00	10.360	11.510	6.27	9.84	-3.57	8.36
IIZw 40	10.10	6.020	< 19.700	6.02	8.59	-2.57	8.09
Mrk 309	167.00	3.430	< 14.800	8.51	9.70	-1.19	8.94
Mrk 750	12.40	0.440	< 0.840	4.47	7.64	-3.17	8.20
VV 523	44.30	2.730	< 11.150	7.20	10.04	-2.84	8.56
IZw 123	10.40	0.300	< 0.640	4.28	7.66	-3.38	7.97